

ORIGINAL RESEARCH

Prognostic prediction and immune landscape analysis based on m6A methylation modification and vasculogenic mimicry in cervical cancer

Lu Zhang¹, Yu Li², Jingrui Yang², Xinmiao Xiong³, Min Kang², Minmin Yu^{2,*}

¹Department of Gynecology, Changzhou Hospital of Traditional Chinese Medicine Affiliated to Nanjing University of Chinese Medicine, 213003 Changzhou, Jiangsu, China

²Department of Gynecology, The Second Hospital of Nanjing, Affiliated to Nanjing University of Chinese Medicine, 210023 Nanjing, Jiangsu, China

³Department of Liver Disease, The Third People's Hospital of Zhenjiang, 212009 Zhenjiang, Jiangsu, China

***Correspondence**

njyy022@njucm.edu.cn
(Minmin Yu)

Abstract

Background: N6-methyladenosine (m6A) modifications are known to play a key role in the development and progression of cancer. Vasculogenic mimicry (VM) is a unique mechanism that can contribute to tumor recurrence and metastasis. However, the specific association between m6A regulators (*MAGs*) and VM-related genes (*VRGs*) in cervical cancer (CC) have yet to be elucidated. **Methods:** Risk signatures were constructed by Univariate Cox regression analysis and least absolute shrinkage and selection operator (LASSO) analysis. The predictive performance of the model was evaluated by Kaplan-Meier survival analysis and receiver operating characteristic (ROC) curves. Patients were divided into high- and low-risk groups based on the median risk score, and differences in key parameters between the two groups were assessed in terms of tumor immune landscape and somatic mutations. **Results:** Based on univariate Cox regression analysis and LASSO regression analyses, we constructed an eight-gene prognostic signature (termed as the mVMscore). High- and low-mVMscore groups, based on median risk scores, were associated with different clinical outcomes and biological characteristics. Survival analysis further demonstrated that patients in the low-mVMscore group had a better survival rate than those in the high-mVMscore group. CIBERSORT and single-sample gene set enrichment analysis (ssGSEA) showed that immune cells were significantly enriched in the high-mVMscore group. Immune scores, estimate scores and stromal scores were lower than those of the low-risk group. **Conclusions:** We constructed a novel prognostic eight-gene signature (mVMscore) based on *MAGs* and *VRGs* which exhibited significant potential to predict the need for immunotherapy in patients with cervical cancer (CC). Collectively, our findings provide a new direction for assessing the prognosis of patients with CC and designing immunotherapy strategies.

Keywords

Cervical cancer; m6A modification; Vasculogenic mimicry; Prognostic signature; Immunotherapy

1. Introduction

Cervical cancer (CC) is one of the leading causes of cancer deaths in women worldwide, ranking fourth in terms of incidence and mortality [1]. Generally, most patients can be treated effectively with standardized therapies, including radiotherapy, chemotherapy and/or surgical resection. However, recurrence and metastasis are still major challenges for patients with locally advanced CC [2, 3]. Therefore, there is an urgent need to identify more reliable diagnostic and prognostic biomarkers for CC.

N6-methyladenosine (m6A) RNA modification is a dynamically reversible form of epigenetic modification that is widespread in eukaryotic cells and is mainly composed of “writers” (e.g., *Methyltransferase-like (METTL) 3/14/16*,

RNA-binding motif protein 15/15B (RBM15/15B), *Vir-like m6A methyltransferase-associated protein (VIRMA*, also known as *KIAA1429*), *Zinc finger CCCH-type containing 13 (ZC3H13)* and *Wilms tumor 1-associated protein (WTAP)*), “readers” (*YTH Domain Family (YTHDF) 1–3* and *YTH Domain-Containing (YTHDC) 1–2* and the *Heterogeneous nuclear ribonucleoprotein (HNRNP) C/A2B1* or *Insulin-like growth factor 2 mRNA-binding proteins (IGF2BP)*) and “erasers” (*Fat mass and obesity-associated protein (FTO)* and *AlkB homologue 5 (ALKBH5)*). These factors are involved in a range of metabolic processes, including RNA splicing, nuclear export and translation [4–7], and can promote the stability of target gene mRNAs to influence gene regulation and the biological functionality of cancer cells [8]. Previous studies confirmed that the aberrant expression of m6A regulators

not only increases the malignant phenotype of tumor cells [9] but also participates in the regulation of tumor immune surveillance [10]. Therefore, the in-depth investigation of m6A methylation modification is expected to provide new concepts for targeted therapy in CC.

Vasculogenic mimicry (VM) is an independent blood perfusion pattern that is independent of the endothelial vasculature and capable of providing a sufficient amount of nutrients for the growth of tumors [11, 12]. Furthermore, VM is a factor that could potentially limit the efficacy of antivascular therapy in some forms of cancer [13–15]. During VM, cancer cells arrange themselves into a tube-like structure that can directly infiltrate into the bloodstream and facilitate the dissemination of cancer cells by invading the extracellular matrix. An increasing number of studies have shown that the formation of VM is closely associated with tumorigenesis, drug resistance and metastasis, including colorectal cancer [16], hepatocellular carcinoma [17], breast cancer [18], glioma [19] and other malignant tumors. Therefore, VM has been recognized as a potential independent indicator of a poor prognosis in patients with cancer [20, 21].

The association between m6A regulators and VM was recently reported in the literature. In this earlier study, the authors found that *METTL3* inhibited Ephrin receptor A2 (EphA2) and Vascular endothelial growth factor A (VEGFA) mRNA degradation in a different IGF2BP-dependent manner and induced VM formation in colorectal cancer by activating the Phosphatidylinositol 3-kinase (PI3K)/AKT/mammalian target of rapamycin (mTOR) and Extracellular signal-related kinases 1/2 (ERK1/2) signaling pathways [22]. Furthermore, *METTL3* is known to enhance the stability of *HOXA* transcript antisense RNA myeloid-specific 1 (*HOTAIRM1*) mRNA and promote VM formation and malignant progression in gliomas [23]. However, it has not been reported whether m6A modification affects the formation of VM formation to promote the progression of CC. Furthermore, whether m6A modification and VM formation are both involved in the regulation of the tumor microenvironment in CC has yet to be established.

In this study, we revealed the complex association between m6A regulators and VM-related genes. We constructed a risk model based on m6A regulators and VM-related genes and comprehensively analyzed the correlation between the risk model and patients with CC in terms of biological function, immune checkpoint genes, the tumor microenvironment and genomic changes, thus providing new insights for assessing the prognosis and immunotherapy of CC.

2. Materials and methods

2.1 Data acquisition

RNA sequencing data (fragments per kilobase of transcript per million fragments mapped (FPKM) values) were downloaded from The Cancer Genome Atlas (TCGA, <https://portal.gdc.cancer.gov/>) database, which included 306 tumor samples and three normal samples. The FPKM values were first converted to transcripts per kilobase million (TPM) values. Next, we downloaded the corresponding clinical

information while excluding samples with a survival time of 0. Finally, 294 patients were included in our analysis. We also downloaded copy number variation data and acquired somatic mutation data from UCSC Xena (<https://xenabrowser.net>).

2.2 Detection of mVM genes

Twenty-eight *MAGs* and 25 *VRGs* were collated from previous literature, thus yielding a total of 53 mVM genes [24–27]. Pearson correlation analysis was then used to assess the correlation between *MAGs* and *VRGs*. Gene interactions were analyzed by the online STRING tool (<https://cn.string-db.org/>) and Cytoscape software version 3.9.0 was used to visualize the correlation results.

2.3 Unsupervised clustering analysis

When investigating the specific role of mVM genes in CC, we determined the optimal number of clusters to cluster patients into different subgroups using the “ConsensusClusterPlus” tool in the R package [28].

2.4 Construction of the mVM prognostic signature

CC patients were randomized into training and validation sets by the “caret” package and used univariate Cox analysis to screen the prognosis-related genes. Subsequent LASSO regression led to the identification of eight key genes thus allowing us to establish a mVM-related prognosis signature. Patients were divided into high- and low-risk groups based on the median risk score (referred to as the mVMscore), and the difference in prognosis between the two groups was assessed using Kaplan-Meier analysis. In addition, time-dependent curves were plotted to evaluate the accuracy of the signature at different periods. The mVMscore, age, grade and TNM (tumor, node, metastasis) staging metrics were incorporated into ROC curves to further evaluate the prognostic predictive ability between mVMscores and clinical factors.

2.5 Functional enrichment analysis and gene set variation analysis (GSVA)

The “clusterProfiler” package was used for Kyoto Encyclopedia of Genes and Genomes (KEGG) analysis to identify functional and pathway enrichment [29]. The “c2.cp.kegg.v7.5.symbols” gene set was downloaded from the Molecular Signatures Database (MSigDB), and differences in biological processes under different mVM modification patterns were determined by GSVA [30].

2.6 Tumor microenvironment and immune infiltration analysis

To quantify tumor-infiltrating immune cells, we used the CIBERSORT algorithm [31] to determine the proportion of infiltrating immune cell types. Single sample gene set enrichment analysis (ssGSEA) was then used to evaluate the abundance of infiltrating immune cells. The “ESTIMATE” tool in the R package was then used to calculate immune scores, stromal scores, estimate scores and tumor purity in

patients with CC [32]. Tumor immune dysfunction and rejection (TIDE) scores were then downloaded from the TIDE database (<http://tide.dfci.harvard.edu/>) and used to evaluate the likelihood of a response to immunotherapy.

2.7 Statistical analysis

All statistical tests were performed in R software version 4.3.1. Pearson's correlation analysis was used to investigate the association between *MAGs* and *VRGs*. Kaplan-Meier survival analysis, with the log-rank test, was then used to compare patients in different subgroups. Statistical significance was set at $p < 0.05$.

3. Results

3.1 Multi-omics characterization of the landscape of m6A regulators in CC

To reveal the regulatory role of m6A modifications in CC, we first explored the genetic changes of 28 m6A regulators. Our analysis showed that the overall mutation frequency of m6A regulators was low, with somatic mutations occurring in 50 of the 289 samples (17.3%); the highest frequencies of mutation (3%) were detected in *Leucine-rich pentatricopeptide repeat containing protein (LRPPRC)*, *ZC3H13* and *YTHDC2* (Fig. 1A). Fig. 1B depicts the majority of m6A regulator copy number deletions, with only *Fragile X mental-retardation protein (FMR1)*, *RBMX*, *HNRNPC*, *METTL3*, *YTHDC1* and *VIRMA* exhibiting amplification. Fig. 1C shows the location of copy number variations for m6A regulators on different chromosomes. In addition, to evaluate the interaction between genetic variations and the expression of m6A regulators, we further analyzed differences in the expression levels of m6A regulators between tumor and normal samples. We found that *METTL16*, *FTO*, *RBM15*, *YTHDF2* and *HNRNPA2B1* exhibited differential expression when compared with normal tissues; specifically, *METTL16* and *FTO* exhibited reduced expression levels in tumor tissues, while *RBM15*, *YTHDF2* and *HNRNPA2B1* exhibited elevated expression levels (Fig. 1D). Pearson correlation analysis confirmed the close correlation between m6A regulators (Fig. 1E). Fig. 1F demonstrates the prognostic value of the three RNA modification species in patients with CC, thus forming a complex regulatory network. Collectively, these results revealed that m6A regulators may play an important role in the progression of CC.

3.2 Association between m6A modifications and VM

A large body of evidence suggests that m6A modifications are involved in regulating the progression of a variety of cancers, and that VM is closely associated with tumor invasion and migration. To investigate whether there is a correlation between m6A modifications and VM, we confirmed the association within *VRGs* by Pearson's correlation analysis; this analysis indicated that *Rho kinase type 1 (ROCK1)* exhibited the strongest correlation with *Mitogen-activated protein kinase 1 (MAPK1)*, with a correlation coefficient of 0.84 (Fig. 2A). In addition, we generated a heatmap which illustrated significant correlations

between m6A modifiers and *VRGs* (Fig. 2B). We also generated a protein-protein interaction (PPI) network which further confirmed the intricate interactions between m6A regulators and *VRGs* (Fig. 2C).

3.3 Identification of mVM molecular patterns and biological function analysis

First, we performed univariate Cox regression analysis on the 53 mVM genes (Supplementary Fig. 1) and selected significant genes ($p < 0.05$) for unsupervised consensus clustering. We found that $k = 3$ was the most appropriate choice when cluster stability increased from $k = 2$ to 9 (Fig. 3A–C); this led to the classification of patients into three subgroups: cluster C1, cluster C2 and cluster C3. When considering the three subgroups, survival analysis showed that cluster C1 had a significantly shorter survival and the worst prognosis (Fig. 3D).

Next, we used GSVA to further compare biological behaviors between the three subgroups. cluster C1 was predominantly enriched in focal adhesion, glycosaminoglycan degradation, glycosaminoglycan biosynthesis, chondroitin sulfate, galactose metabolism and the nod-like receptor signaling pathway. cluster C2 was significantly enriched in the linoleic acid metabolism pathway while cluster C3 was associated with metabolic or biosynthetic activation phenotypes (Supplementary Fig. 2A–C). Analysis of immune cell infiltration further showed that cluster C1 was mainly enriched in innate immune cells, such as $\gamma\delta$ T cells, mast cells, neutrophils, regulatory T cells and Type 2 T helper cells. Activated B cells accounted for the largest proportion of cells in cluster C2, while cluster C3 featured the highest number of immature dendritic cells (Fig. 3E).

3.4 Construction and validation of prognostic signature

With the purpose of better predicting the clinical prognosis based on mVM genes, patients with CC in the TCGA database were randomly divided into a training set and a validation set for model construction and validation. First, we performed univariate Cox regression analysis on 53 mVM genes (Supplementary Fig. 1) and identified 14 prognosis-related genes ($p < 0.05$). To improve the predictive effect, we used the LASSO-Cox regression algorithm for further screening; this strategy ultimately identified eight prognostic genes (Fig. 4A,B). Kaplan-Meier analysis demonstrated that high expression levels of all eight genes identified by LASSO analysis were significantly associated with a poor patient prognosis (Supplementary Fig. 3). In addition, we constructed a prognostic signature by calculating the risk score for each patient, which we defined as the mVMscore. Patients with CC were then categorized into low-risk and high-risk groups based on the median mVMscore. Fig. 4C–E shows the mVMscore, survival time, live status and a heatmap of mVM genes expression in CC. Kaplan-Meier survival curves further showed that the high mVMscore group had a worse prognosis than the low mVMscore group, both in the training group (Supplementary Fig. 4A), the validation group (Supplementary Fig. 4B), and in the entire cohort (Fig. 5A).

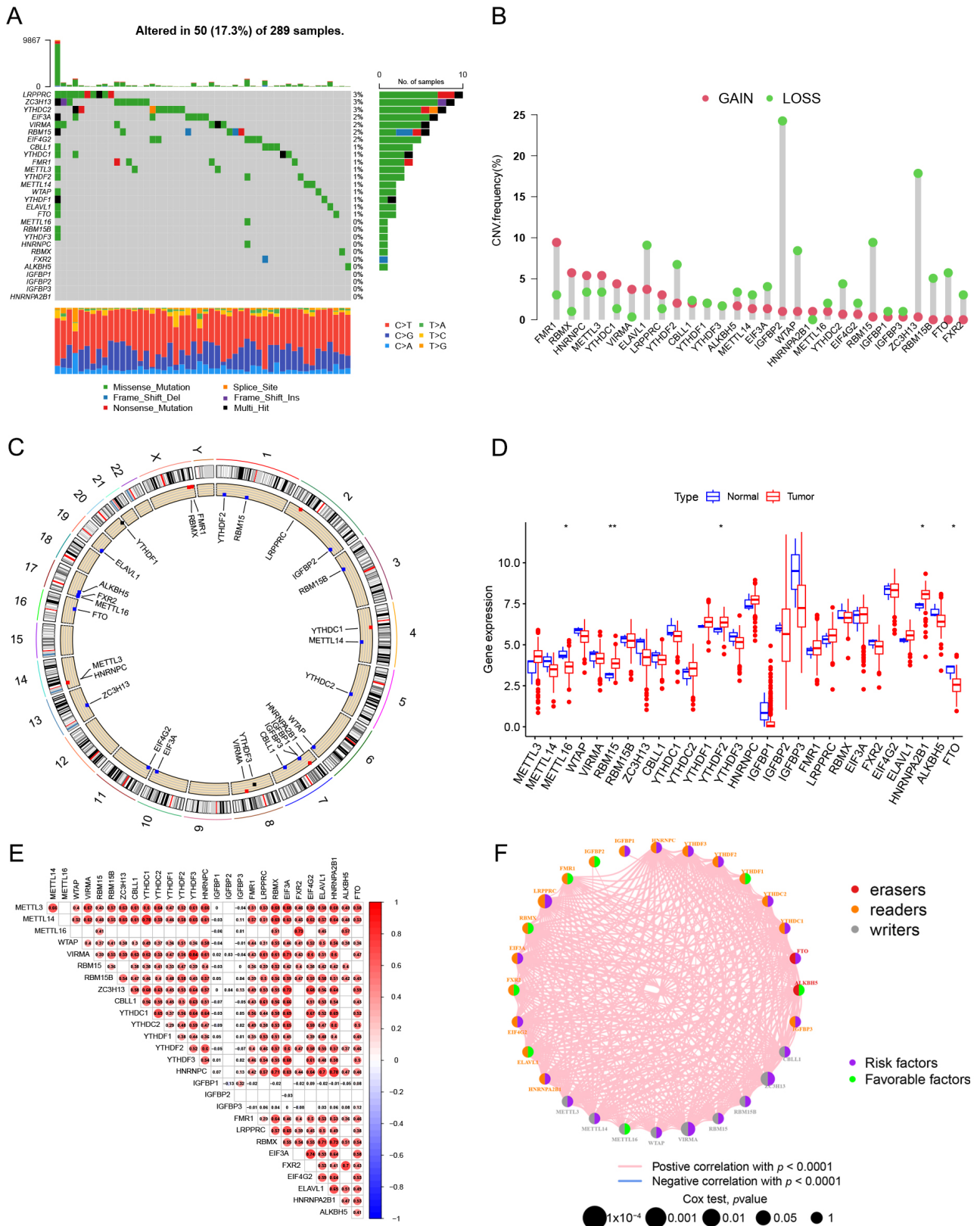


FIGURE 1. Multi-omics characterization landscape of m6A regulators in cervical cancer. (A) The mutation landscape of 28 m6A regulators. (B) Copy number variation alteration frequency of m6A regulators. (C) The location of CNV alteration of m6A regulators on chromosomes. (D) Differential expression of m6A regulators in tumor and normal samples. * $p < 0.05$, ** $p < 0.01$. (E) Pearson correlation analysis reveals positive and negative correlations among m6A regulators. (F) Prognostic network diagram of the three RNA modification species. The left half of circle in different colors represents different RNA modification types. Lines between m6A regulators represent their positive/negative correlations. The size of the circles represents the relationship between m6A regulators and survival. The larger the circle the more likely it is to be a prognosis-related gene.

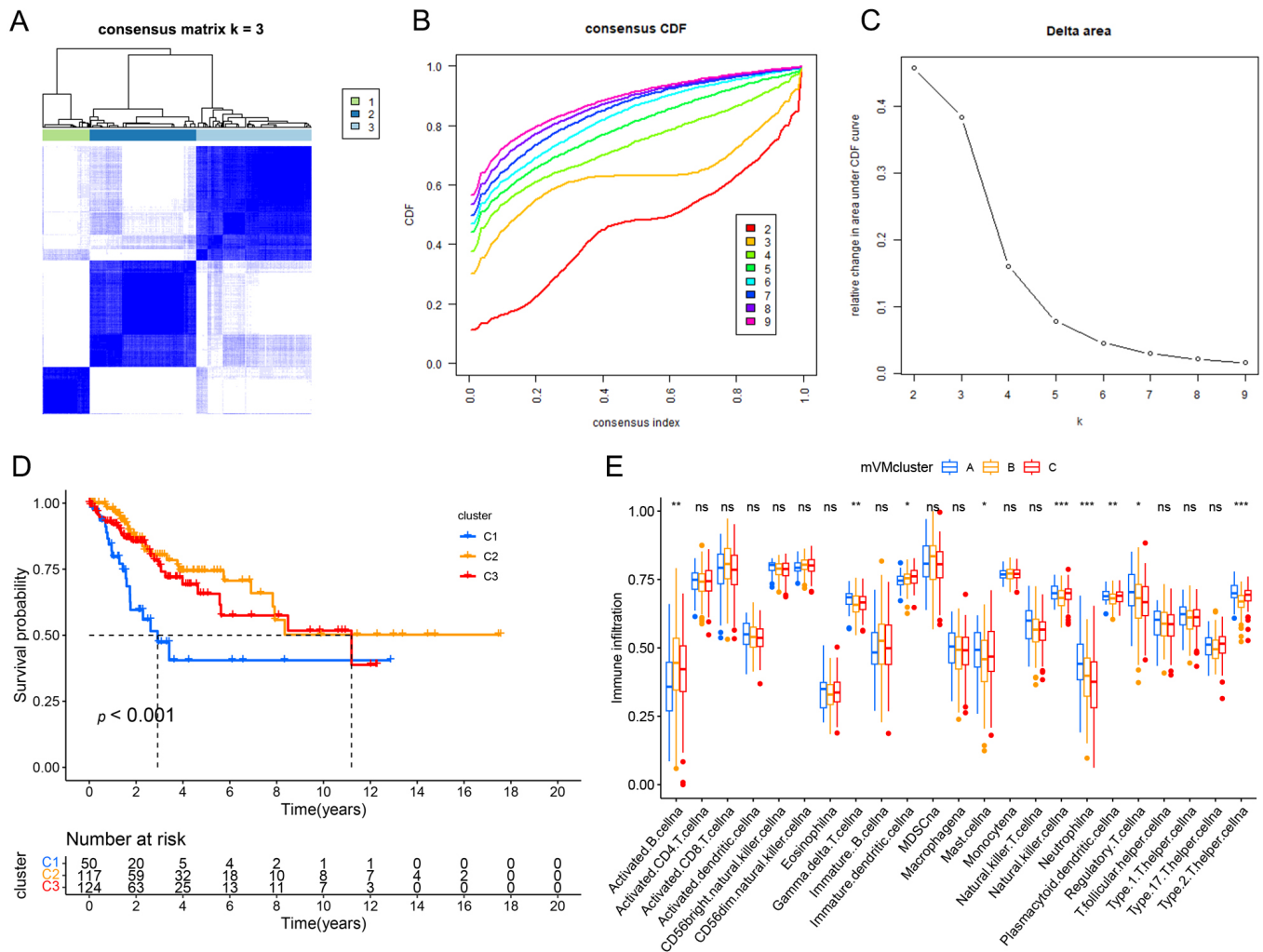


FIGURE 3. Recognition of mVM genes modification patterns. (A) Consensus clustering matrix at $k = 3$. (B) Cumulative Distribution Function (CDF) curve for consensus clustering analysis at $k = 2-9$. (C) Relative change in area under the CDF curve at $k = 2-9$. (D) Survival analysis of different clusters by Kaplan-Meier. (E) The abundance of immune-infiltrating cells in the three clusters. * $p < 0.05$, ** $p < 0.01$, *** $p < 0.001$.

death status than in patients with survival status (Fig. 5F). Subsequently, we investigated the association between Tumour mutation burden (TMB) and mVMscore and found that patients in the high TMB group had a significantly better prognosis (Fig. 5G). When the high TMB group was combined with the low mVMscore group, we found that survival was significantly better than for the other groups (Fig. 5H).

Next, we compared somatic mutation frequencies between the high mVMscore and low mVMscore subgroups and found that overall mutation frequencies did not differ significantly between these two groups. The most common type of mutation was nonsense mutations; furthermore, the somatic mutation rates of *TTN* (36% vs. 22%) and *Phosphatidylinositol-4,5-bisphosphate 3-kinase catalytic subunit alpha (PIK3CA)* (30% vs. 23%) were significantly higher in the high mVMscore subgroup (Fig. 6A) than in the low mVMscore subgroup (Fig. 6B). In addition, we also demonstrated that the top 20 mutated genes were significantly less frequent in the high mVMscore group (Fig. 6C), but were more frequent in the low mVMscore group (Fig. 6D).

3.6 Correlation between mVMscore and the tumor immune landscape

To enhance our understanding of the tumor microenvironment, we next assessed the abundance of immune-infiltrating cells in the tumor microenvironment by performing CIBERSORT and ssGSEA analyses. These analysis showed that immune cells were significantly enriched in the high-risk group, including activated B cells, activated cytotoxic CD8 T cells, eosinophils, immature B cells, immature dendritic cells, myeloid-derived suppressor cells (MDSCs), macrophages, regulated immature B cells, regulatory T (Treg) cells, follicular helper T (Tfh) cells, type 1 helper T (Th1) cells and natural killer (NK) cells (Fig. 7A,B). Based on the ESTIMATE algorithm, we then analyzed the differences between stromal and immune cells in the high and low-mVMscore groups. Analysis showed that the immune score, estimated score, and stromal score were higher in the low-risk group than in the high-risk group (Fig. 7C). TIDE scores were higher in the low-mVMscore group (Fig. 7D), thus indicating that immune escape was more

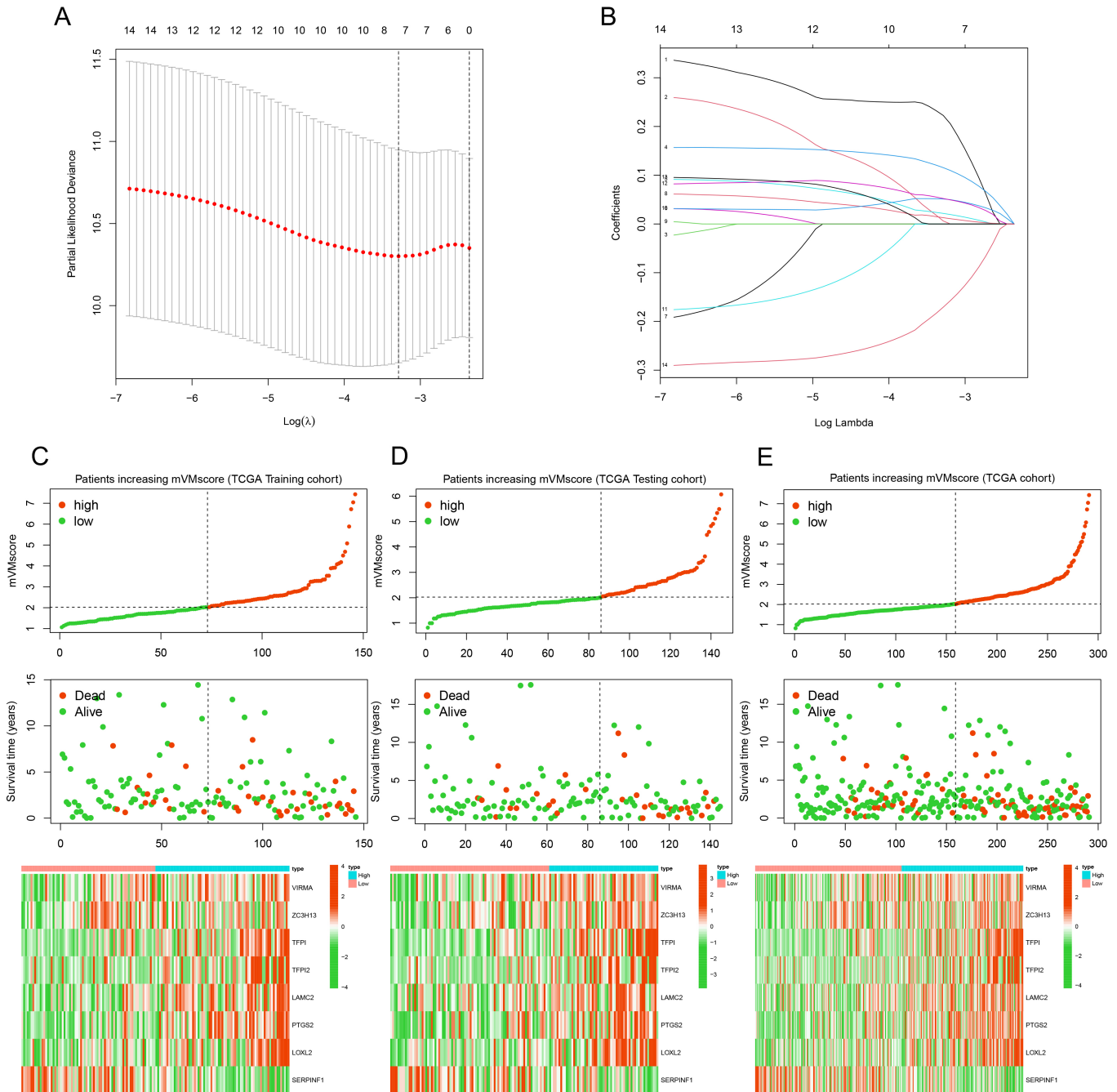


FIGURE 4. Construction of a prognosis signature base on mVM genes. (A,B) LASSO Cox analysis identified eight prognosis-related genes. (C–E) Distribution of mVMscore, survival status of CC patients and heatmap expression of characteristic gene expression in the training cohort (C), testing cohort (D) and entire TCGA cohort (E).

likely to occur in patients in the low-risk group, and that the efficacy of immunotherapy was greatly reduced. Therefore, we also analyzed the expression levels of immune checkpoint genes, including *Programmed death-ligand 1 (PD-L1)*, *Programmed cell death protein 1 (PD-1)* and *CTL-associated antigen 4 (CTLA4)*. Analysis showed that the expression levels of immune checkpoint genes were up-regulated in all of the low-mVMscore groups (Fig. 7E). These findings suggested that immunotherapy efficacy was weaker in the low-risk population, and that the benefit of immunotherapy may be greater in the high-mVMscore group. Collectively, our results suggest that the mVMscore has great potential for assessing the tumor

microenvironment, immune function, and immunotherapy in patients with CC.

4. Discussion

Despite significant advances in CC screening and vaccination over recent years, recurrence and metastasis remain important factors that affect the survival of patients [33]. Previous studies have demonstrated that m6A methylation modification promotes both tumorigenesis and metastasis [34, 35]; furthermore, VM is now considered as a strong causative factor for tumor recurrence as well as shorter patient survival times [36, 37]. A few studies have reported the association between m6A

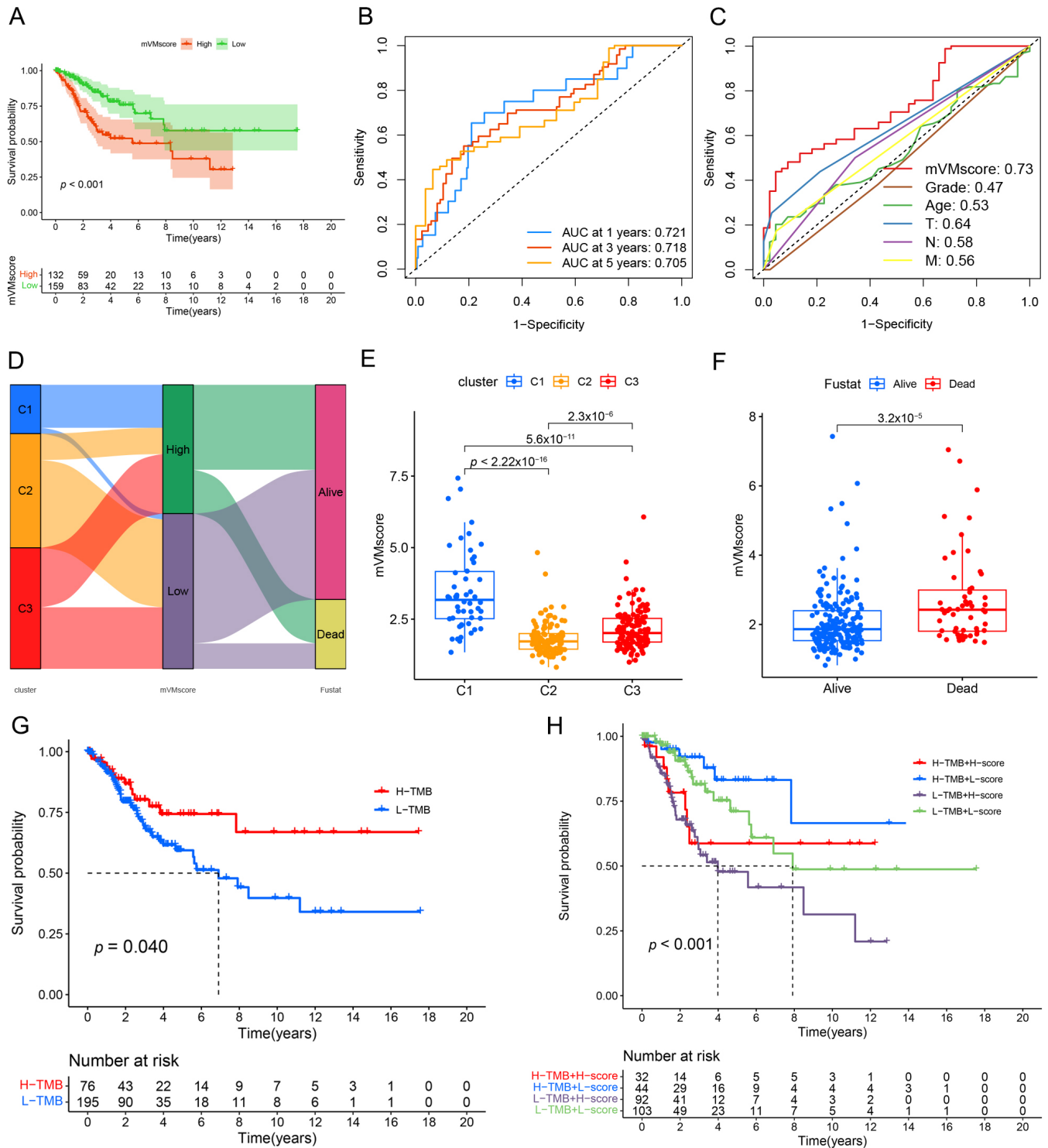


FIGURE 5. Analysis of mVMscore correlation with clinical traits and somatic mutations. (A) Kaplan-Meier curves of the mVMscore in the entire TCGA dataset. (B) Time-dependent ROC curve of the mVMscore prognostic signature for 1-, 3- and 5-year overall survival (OS) of CC patients in the entire TCGA dataset. (C) ROC curve analysis of the mVMscore and clinicopathological parameters (grade, age, T stage, N stage and M stage) for 5-year OS. (D) The alluvial diagram depicted the changes of clusters, mVMscore and survival status. (E) Comparison of mVMscore among different clusters. (F) Comparison of mVMscore between different survival states. (G) Kaplan-Meier curves for high-TMB vs. low-TMB groups. (H) Kaplan-Meier survival analysis for patients with different expression levels of mVMscore & TMB.

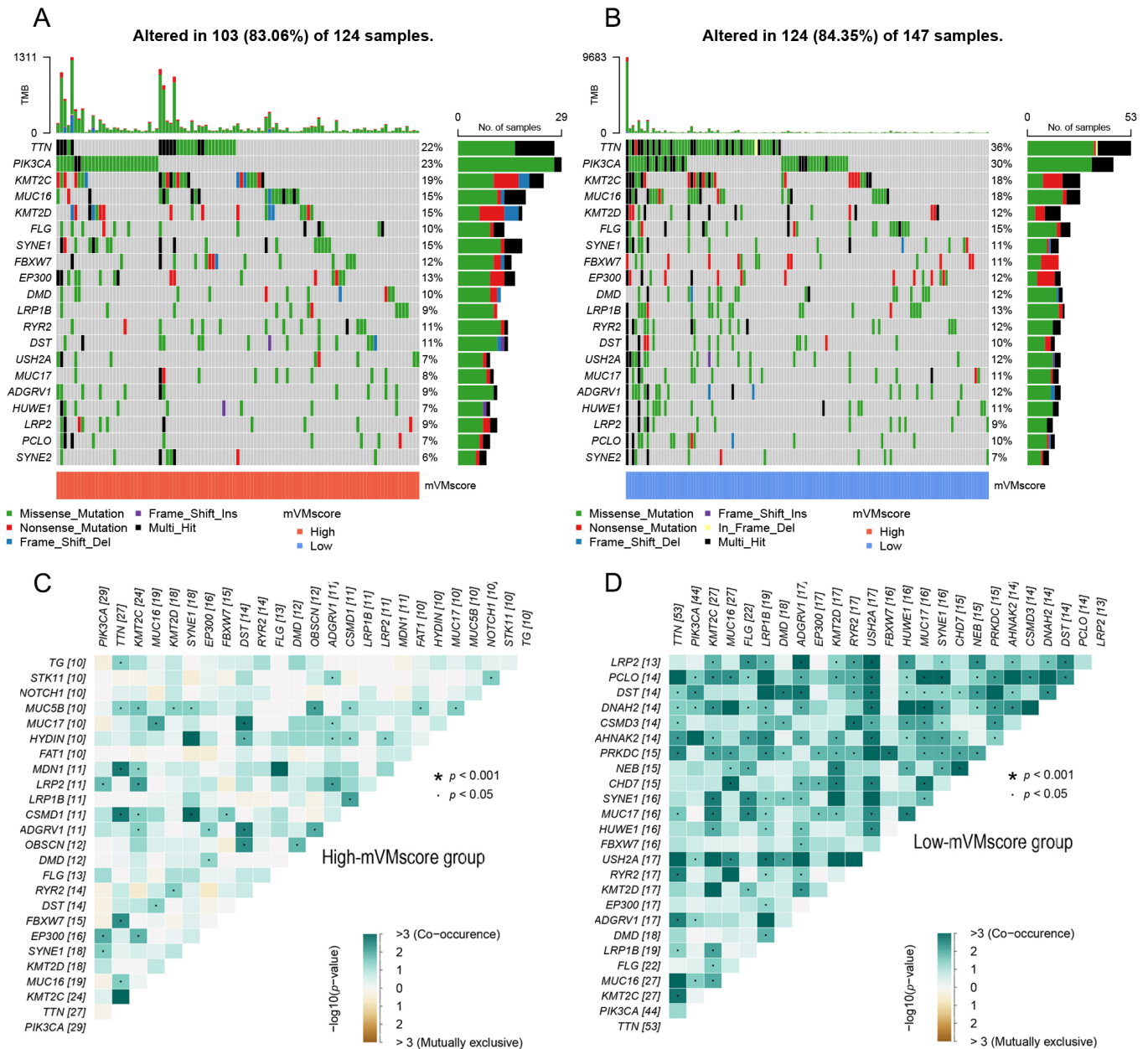


FIGURE 6. Comparison of somatic mutations among different subgroups. (A) The mutation alteration in high-risk group. (B) The mutation alteration in low-risk group. (C) Correlation of mutated genes in high mVMscore groups. (D) Correlation of mutated genes in low mVMscore groups.

regulators and VM [38, 39]. However, the role of both m6A methylation and VM in CC has not been reported.

VM has attracted significant attention since it was first discovered. The presence of VM has been reported in a variety of malignant tumors and is strongly associated with a poor patient prognosis. Furthermore, VM is considered to be a characteristic manifestation of highly aggressive and metastatic tumor cells. A previous meta-analysis indicated that VM exerts significant effect on clinicopathological features [40], such as tumor histological differentiation, metastasis and clinical staging, thus suggesting that VM-positive patients have poorer survival outcomes. m6A methylation modification is one of the most commonly investigated forms of RNA modification. Evidence suggests that VM formation is regulated by m6A methylation modification. Liu *et al.*

[41] reported that *Insulin-like growth factor-binding protein 2 (IGFBP2)* enhanced the expression of *Vascular endothelial cadherin (CD144)* and *Matrix Metalloproteinase 2 (MMP2)* through the Focal Adhesion Kinase (FAK)/ERK/Specificity protein-1 (SP1) signaling pathway, which then plays a role in the positive regulation of VM formation in gliomas. In another study, Qiao *et al.* [42] found that *METTL3* enhances the translation efficiency of Yes-associated protein isoform 1 (YAP1) mRNA, which mediates the occurrence of VM in hepatocellular carcinoma. In addition, the demethylase *ALKBH5* has also been shown to be involved in the progression of VM in gliomas; in addition, tissues with high expression levels of *ALKBH5* had a higher rate of VM positivity [43]. These recent reports confirm the feasibility of our current findings. In our study, the combination of Pearson's correlation analysis

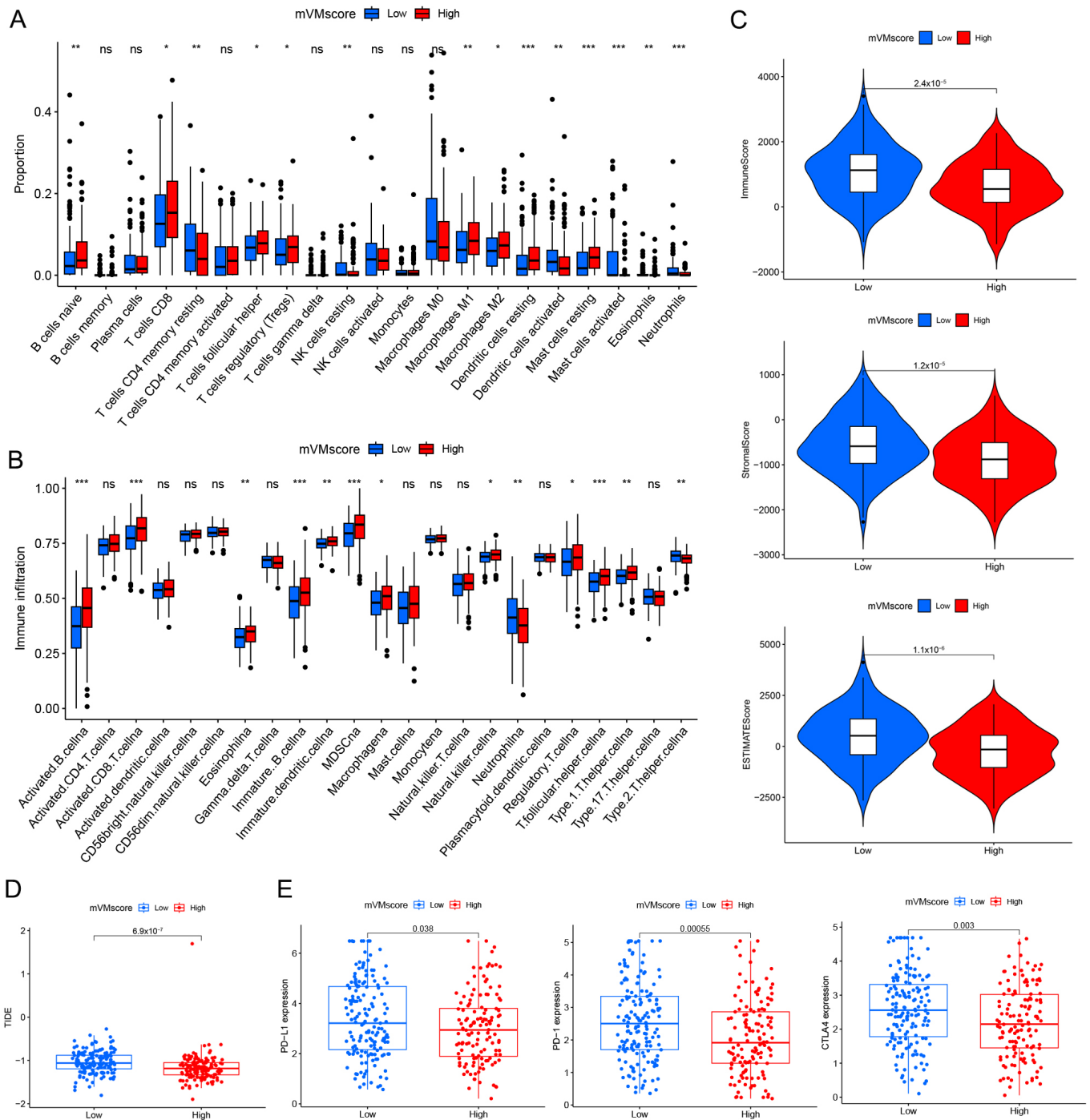


FIGURE 7. Potential for predicting immunotherapeutic response in mVM signature. (A) Differences in infiltration of immune cell types between the two subgroups. (B) The infiltrating levels of different immune cell types. (C) ESTIMATE was performed to compare immune scores, stromal scores, tumor purity and estimate scores in two groups. (D) TIDE prediction difference in the high- and low-risk patients. (E) Violin plot depicted the expression of checkpoint genes in the high- and low-mVMscore groups. * $p < 0.05$, ** $p < 0.01$, *** $p < 0.001$.

and PPI network construction revealed the close interaction between m6A regulators and VM-related genes. This finding provides further possibilities for therapeutic options in CC.

This represents the first study to investigate the association between m6A modification and VM; our aim was to improve the accuracy and specificity of prognostic modeling by combining two prognostic biomarkers. Furthermore, the expression patterns of mVM genes were identified by

consensus clustering; this resulted in the classification of CC patients into three subtypes. Prognostic analyses revealed significant differences between the three subtypes; cluster C1 had the worst prognosis. Eight prognostic genes (*VIRMA*, *ZC3H13*, *Tissue factor pathway inhibitor (TFPI)*, *TFPI2*, *Laminin gamma2 (LAMC2)*, *Prostaglandin-endoperoxide synthase 2 (PTGS2)*, *Lysyl oxidase-like 2 (LOXL2)* and *Serpin peptidase inhibitor-clade F-member 1 (SERPINF1)*) were

then identified based on univariate Cox regression analysis and LASSO regression analysis. Of these, *ZC3H13* has been shown to regulate Centromere protein K (CENPK) mRNA stability to promote the stemness and chemoresistance of CC [44]. A retrospective trial found that patients with high levels of *VIRMA* protein expression had shorter overall survival [45]. *TFPI2*, as an oncogene, is involved in the regulation of apoptosis in CC [46]. Migration of squamous cell carcinoma cells, including cervical cancer, is diminished when *LAMC2* transcription is inhibited. *LOXL2* enhances the ability of CC cells to proliferate, invade and migrate, and inhibits apoptosis by inducing Epithelial-mesenchymal-transition (EMT) both *in vivo* and *in vitro* [47]. *PTGS2*, also known as *Cyclooxygenase 2 (COX2)*, is abnormally elevated during inflammation, and Human papilloma viruses (HPV) may induce cervical carcinogenesis through the *PTGS2* inflammatory pathway [48]. However, the biological function of *SERPINF1* has been rarely reported in CC. And we found that only low expression of *SERPINF1* gene was significantly associated with short overall survival of patients in the survival analysis of eight prognostic genes, so further experimental studies are now needed to investigate the function of *SERPINF1*.

The tumor microenvironment has been the focus of significant research due to its complex role in promoting the invasion, metastasis and distant dissemination of CC. The incalculable translational potential of the tumor microenvironment holds significant promise for immunotherapeutic diversity in CC [49]. In the present study, we investigated the proportion of tumor immune cell infiltration between high/low risk groups by performing CIBERSORT and ssGSEA analysis. Analysis revealed a high degree of immune cell infiltration in the high-risk group, including activated B cells, activated CD8 T cells, eosinophils, immature dendritic cells, myeloid-derived suppressor cells (MDSCs), macrophages, neutrophils, regulatory T (Treg) cells, follicular helper T (Tfh) cells, type 1 helper T (Th1) cells, activated B cells, CD8 T cells, eosinophils and NK cells. Notably, MDSCs and Treg cells were enriched in the high-risk group, which may be one of the reasons for the poorer prognosis of patients in the high-risk group [50, 51]. The infiltrations of activated B cells, CD8 T cells and eosinophils were shown to be associated with a better prognosis in CC, which is in contrast to our results [52, 53]. Interestingly, in colorectal cancer the expression level of anti-tumor immune cells was elevated in the high-risk group, including CD8⁺ T cells and B cells, which is the same as our findings [54]. The bias that causes this result may be due to the presence of tumor heterogeneity. In addition, we found that the low-risk group was associated with high immunity scores and upregulated expression levels of immune checkpoint genes (*PD-L1*, *PD-L1*, *CTLA4*). Furthermore, the TIDE score was higher in the low-risk group, thus indicating that the low-risk group was more prone to immunosuppression. Therefore, identifying and targeting different molecular subgroups of CC offers hope for the development of efficient therapeutic strategies.

However, there are some limitations to this study that need to be considered. First, we only used data from the TCGA database for internal validation; this may have influenced the generalization and stability of our new model. Second, the genes identified herein also need to be validated in clinical

studies to improve the accuracy of clinical prediction. Finally, our analysis was limited by the normal tissue sample size of the TCGA database, the statistical results may be biased; more datasets are required for in-depth validation.

5. Conclusions

In this study, we constructed a risk signature, based on m6A regulators and VM-related genes, that demonstrated good clinical prediction ability and immunotherapy value. This model has significant potential for guiding immunotherapy in patients with CC.

AVAILABILITY OF DATA AND MATERIALS

The data presented in this study are available on reasonable request from the corresponding author.

AUTHOR CONTRIBUTIONS

LZ and MMY—designed the study and performed the research. YL and XM—analyzed the data and wrote the manuscript. JRY—assisted in the completion of the paper. MK—Collection and assembly of data. All authors contributed to editorial changes in the manuscript. All authors read and approved the final manuscript.

ETHICS APPROVAL AND CONSENT TO PARTICIPATE

Not applicable.

ACKNOWLEDGMENT

Not applicable.

FUNDING

This work was supported by the National Natural Science Foundation of China-Youth Science Foundation Project (82002640); the Natural Science Research Project of Jiangsu Province University (20KJB320028) and the Project of Nanjing University of Traditional Chinese Medicine (KYCX23_2103).

CONFLICT OF INTEREST

The authors declare no conflict of interest.

SUPPLEMENTARY MATERIAL

Supplementary material associated with this article can be found, in the online version, at <https://oss.ejgo.net/files/article/1922893993217015808/attachment/Supplementary%20material.docx>.

REFERENCES

- [1] Sung H, Ferlay J, Siegel RL, Laversanne M, Soerjomataram I, Jemal A, *et al.* Global cancer statistics 2020: GLOBOCAN estimates of incidence and mortality worldwide for 36 cancers in 185 countries. *CA: A Cancer Journal for Clinicians.* 2021; 71: 209–249.
- [2] Gennigens C, Jerusalem G, Lapaille L, De Cuyper M, Strel S, Kridelka F, *et al.* Recurrent or primary metastatic cervical cancer: current and future treatments. *ESMO Open.* 2022; 7: 100579.
- [3] Mayadev JS, Ke G, Mahantshetty U, Pereira MD, Tarnawski R, Toita T. Global challenges of radiotherapy for the treatment of locally advanced cervical cancer. *International Journal of Gynecological Cancer.* 2022; 32: 436–445.
- [4] Wang Z, Zhou J, Zhang H, Ge L, Li J, Wang H. RNA m⁶A methylation in cancer. *Molecular Oncology.* 2023; 17: 195–229.
- [5] Li S, Qi Y, Yu J, Hao Y, He B, Zhang M, *et al.* Nuclear aurora kinase a switches m⁶A reader YTHDC1 to enhance an oncogenic RNA splicing of tumor suppressor RBM4. *Signal Transduction and Targeted Therapy.* 2022; 7: 97.
- [6] Xu P, Yang J, Chen Z, Zhang X, Xia Y, Wang S, *et al.* N⁶-methyladenosine modification of CENPF mRNA facilitates gastric cancer metastasis via regulating FAK nuclear export. *Cancer Communications.* 2023; 43: 685–705.
- [7] Wilinski D, Dus M. N⁶-adenosine methylation controls the translation of insulin mRNA. *Nature Structural & Molecular Biology.* 2023; 30: 1260–1264.
- [8] Yin H, Chen L, Piao S, Wang Y, Li Z, Lin Y, *et al.* M6A RNA methylation-mediated RMRP stability renders proliferation and progression of non-small cell lung cancer through regulating TGFBR1/SMAD2/SMAD3 pathway. *Cell Death & Differentiation.* 2023; 30: 605–617.
- [9] Wang JJ, Chen DX, Zhang Y, Xu X, Cai Y, Wei WQ, *et al.* Elevated expression of the RNA-binding protein IGF2BP1 enhances the mRNA stability of INHBA to promote the invasion and migration of esophageal squamous cancer cells. *Experimental Hematology & Oncology.* 2023; 12: 75.
- [10] Wan W, Ao X, Chen Q, Yu Y, Ao L, Xing W, *et al.* METTL3/IGF2BP3 axis inhibits tumor immune surveillance by upregulating N⁶-methyladenosine modification of PD-L1 mRNA in breast cancer. *Molecular Cancer.* 2022; 21: 60.
- [11] Sun B, Zhang D, Zhao N, Zhao X. Epithelial-to-endothelial transition and cancer stem cells: two cornerstones of vasculogenic mimicry in malignant tumors. *Oncotarget.* 2017; 8: 30502–30510.
- [12] Wei X, Chen Y, Jiang X, Peng M, Liu Y, Mo Y, *et al.* Mechanisms of vasculogenic mimicry in hypoxic tumor microenvironments. *Molecular Cancer.* 2021; 20: 7.
- [13] Angara K, Borin TF, Rashid MH, Lebedyeva I, Ara R, Lin PC, *et al.* Corrigendum to “CXCR2-expressing tumor cells drive vascular mimicry in antiangiogenic therapy-resistant glioblastoma” neoplasia, October 2018, volume 20, issue 10, pages 1070–1082. *Neoplasia: An International Journal for Oncology Research.* 2019; 21: 156–157.
- [14] Xu Y, Li Q, Li XY, Yang QY, Xu WW, Liu GL. Short-term anti-vascular endothelial growth factor treatment elicits vasculogenic mimicry formation of tumors to accelerate metastasis. *Journal of Experimental & Clinical Cancer Research.* 2012; 31: 16.
- [15] Cannell IG, Sawicka K, Pearsall I, Wild SA, Deighton L, Pearsall SM, *et al.* FOXC2 promotes vasculogenic mimicry and resistance to anti-angiogenic therapy. *Cell Reports.* 2023; 42: 112791.
- [16] Huang S, Wang X, Zhu Y, Wang Y, Chen J, Zheng H. SOX2 promotes vasculogenic mimicry by accelerating glycolysis via the lncRNA AC005392.2-GLUT1 axis in colorectal cancer. *Cell Death & Disease.* 2023; 14: 791.
- [17] Shi Y, Shang J, Li Y, Zhong D, Zhang Z, Yang Q, *et al.* ITGA5 and ITGB1 contribute to Sorafenib resistance by promoting vasculogenic mimicry formation in hepatocellular carcinoma. *Cancer Medicine.* 2023; 12: 3786–3796.
- [18] Jung E, Lee YH, Ou S, Kim TY, Shin SY. EGR1 Regulation of vasculogenic mimicry in the MDA-MB-231 triple-negative breast cancer cell line through the upregulation of KLF4 expression. *International Journal of Molecular Sciences.* 2023; 24: 14375.
- [19] Huang Y, Zhu C, Liu P, Ouyang F, Luo J, Lu C, *et al.* LICAM promotes vasculogenic mimicry formation by miR-143-3p-induced expression of hexokinase 2 in glioma. *Molecular Oncology.* 2023; 17: 664–685.
- [20] Provance OK, Oria VO, Tran TT, Caulfield JI, Zito CR, Aguirre-Ducler A, *et al.* Vascular mimicry as a facilitator of melanoma brain metastasis. *Cellular and Molecular Life Sciences.* 2024; 81: 188.
- [21] Sabazade S, Gill V, Herrspiegel C, Stalhammar G. Vasculogenic mimicry correlates to presenting symptoms and mortality in uveal melanoma. *Journal of Cancer Research and Clinical Oncology.* 2022; 148: 587–597.
- [22] Liu X, He H, Zhang F, Hu X, Bi F, Li K, *et al.* m6A methylated EphA2 and VEGFA through IGF2BP2/3 regulation promotes vasculogenic mimicry in colorectal cancer via PI3K/AKT and ERK1/2 signaling. *Cell Death & Disease.* 2022; 13: 483.
- [23] Wu Z, Wei N. METTL3-mediated HOTAIRM1 promotes vasculogenic mimicry in glioma via regulating IGFBP2 expression. *Journal of Translational Medicine.* 2023; 21: 855.
- [24] Xiong J, Lian W, Zhao R, Gao K. METTL3/MALAT1/ELAVL1 axis promotes tumor growth in ovarian cancer. *OncoTargets and Therapy.* 2024; 17: 85–97.
- [25] Di Timoteo G, Dattilo D, Centron-Broco A, Colantoni A, Guarnacci M, Rossi F, *et al.* Modulation of circRNA metabolism by m⁶A modification. *Cell Reports.* 2020; 31: 107641.
- [26] Wang J, Xia W, Huang Y, Li H, Tang Y, Li Y, *et al.* A vasculogenic mimicry prognostic signature associated with immune signature in human gastric cancer. *Frontiers in Immunology.* 2022; 13: 1016612.
- [27] Wen T, Li T, Xu Y, Zhang Y, Pan H, Wang Y. The role of m6A epigenetic modifications in tumor coding and non-coding RNA processing. *Cell Communication and Signaling.* 2023; 21: 355.
- [28] Wilkerson MD, Hayes DN. ConsensusClusterPlus: a class discovery tool with confidence assessments and item tracking. *Bioinformatics.* 2010; 26: 1572–1573.
- [29] Yu G, Wang LG, Han Y, He QY. clusterProfiler: an R package for comparing biological themes among gene clusters. *OMICS.* 2012; 16: 284–287.
- [30] Hanzelmann S, Castelo R, Guinney J. GSEA: gene set variation analysis for microarray and RNA-seq data. *BMC Bioinformatics.* 2013; 14: 7.
- [31] Newman AM, Liu CL, Green MR, Gentles AJ, Feng W, Xu Y, *et al.* Robust enumeration of cell subsets from tissue expression profiles. *Nature Methods.* 2015; 12: 453–457.
- [32] Yoshihara K, Shahmoradgoli M, Martinez E, Vegesna R, Kim H, Torres-Garcia W, *et al.* Inferring tumour purity and stromal and immune cell admixture from expression data. *Nature Communications.* 2013; 4: 2612.
- [33] Li Y, Chen Z, Wang X, Li X, Zhou J, Zhang Y. Clinical outcomes observation in stage IIB–IIIB cervical cancer treated by adjuvant surgery following concurrent chemoradiotherapy. *BMC Cancer.* 2021; 21: 442.
- [34] Hu Y, Gong C, Li Z, Liu J, Chen Y, Huang Y, *et al.* Demethylase ALKBH5 suppresses invasion of gastric cancer via PKMYT1 m6A modification. *Molecular Cancer.* 2022; 21: 34.
- [35] Xu Y, Song M, Hong Z, Chen W, Zhang Q, Zhou J, *et al.* The N⁶-methyladenosine METTL3 regulates tumorigenesis and glycolysis by mediating m6A methylation of the tumor suppressor LATS1 in breast cancer. *Journal of Experimental & Clinical Cancer Research.* 2023; 42: 10.
- [36] Ge H, Luo H. Overview of advances in vasculogenic mimicry—a potential target for tumor therapy. *Cancer Management and Research.* 2018; 10: 2429–2437.
- [37] Zhang Y, Bai J, Cheng R, Zhang D, Qiu Z, Liu T, *et al.* TAZ promotes vasculogenic mimicry in gastric cancer through the upregulation of TEAD4. *Journal of Gastroenterology and Hepatology.* 2022; 37: 714–726.
- [38] Liu M, Ruan X, Liu X, Dong W, Wang D, Yang C, *et al.* The mechanism of BUD13 m6A methylation mediated MBNL1-phosphorylation by CDK12 regulating the vasculogenic mimicry in glioblastoma cells. *Cell Death & Disease.* 2022; 13: 1017.
- [39] Cheng B, Xie M, Zhou Y, Li T, Liu W, Yu W, *et al.* Vascular mimicry induced by m⁶A mediated IGFL2-AS1/AR axis contributes to pazopanib resistance in clear cell renal cell carcinoma. *Cell Death Discovery.* 2023; 9: 121.
- [40] Yang JP, Liao YD, Mai DM, Xie P, Qiang YY, Zheng LS, *et al.* Tumor vasculogenic mimicry predicts poor prognosis in cancer patients: a meta-

- analysis. *Angiogenesis*. 2016; 19: 191–200.
- [41] Liu Y, Li F, Yang YT, Xu XD, Chen JS, Chen TL, *et al.* IGFBP2 promotes vasculogenic mimicry formation via regulating CD144 and MMP2 expression in glioma. *Oncogene*. 2019; 38: 1815–1831.
- [42] Qiao K, Liu Y, Xu Z, Zhang H, Zhang H, Zhang C, *et al.* RNA m6A methylation promotes the formation of vasculogenic mimicry in hepatocellular carcinoma via Hippo pathway. *Angiogenesis*. 2021; 24: 83–96.
- [43] Tao M, Li X, He L, Rong X, Wang H, Pan J, *et al.* Decreased RNA m⁶A methylation enhances the process of the epithelial mesenchymal transition and vasculogenic mimicry in glioblastoma. *American Journal of Cancer Research*. 2022; 12: 893–906.
- [44] Lin X, Wang F, Chen J, Liu J, Lin YB, Li L, *et al.* N⁶-methyladenosine modification of CENPK mRNA by ZC3H13 promotes cervical cancer stemness and chemoresistance. *Military Medical Research*. 2022; 9: 19.
- [45] Condic M, Ralser DJ, Klumper N, Ellinger J, Qureishi M, Egger EK, *et al.* Comprehensive analysis of N⁶-Methyladenosine (m⁶A) writers, erasers, and readers in cervical cancer. *International Journal of Molecular Sciences*. 2022; 23: 7165.
- [46] Zhang Q, Zhang Y, Wang SZ, Wang N, Jiang WG, Ji YH, *et al.* Reduced expression of tissue factor pathway inhibitor-2 contributes to apoptosis and angiogenesis in cervical cancer. *Journal of Experimental & Clinical Cancer Research*. 2012; 31: 1.
- [47] Peng T, Lin S, Meng Y, Gao P, Wu P, Zhi W, *et al.* LOXL2 small molecule inhibitor restrains malignant transformation of cervical cancer cells by repressing LOXL2-induced epithelial-mesenchymal transition (EMT). *Cell Cycle*. 2022; 21: 1827–1841.
- [48] Cardoso LP, de Sousa SO, Gusson-Zanetoni JP, de Melo Moreira Silva LL, Frigieri BM, Henrique T, *et al.* Piperine reduces neoplastic progression in cervical cancer cells by downregulating the cyclooxygenase 2 pathway. *Pharmaceuticals*. 2023; 16: 103.
- [49] De Nola R, Menga A, Castegna A, Loizzi V, Ranieri G, Cicinelli E, *et al.* The crowded crosstalk between cancer cells and stromal microenvironment in gynecological malignancies: biological pathways and therapeutic implication. *International Journal of Molecular Sciences*. 2019; 20: 2401.
- [50] Jianyi D, Haili G, Bo Y, Meiqin Y, Baoyou H, Haoran H, *et al.* Myeloid-derived suppressor cells cross-talk with B10 cells by BAFF/BAFF-R pathway to promote immunosuppression in cervical cancer. *Cancer Immunology, Immunotherapy*. 2023; 72: 73–85.
- [51] Ni H, Zhang H, Li L, Huang H, Guo H, Zhang L, *et al.* T cell-intrinsic STING signaling promotes regulatory T cell induction and immunosuppression by upregulating FOXP3 transcription in cervical cancer. *Journal for Immunotherapy of Cancer*. 2022; 10: e005151.
- [52] Shen X, Wang C, Li M, Wang S, Zhao Y, Liu Z, *et al.* Identification of CD8⁺ T cell infiltration-related genes and their prognostic values in cervical cancer. *Frontiers in Oncology*. 2022; 12: 1031643.
- [53] Yu S, Li X, Zhang J, Wu S. Development of a novel immune infiltration-based gene signature to predict prognosis and immunotherapy response of patients with cervical cancer. *Frontiers in Immunology*. 2021; 12: 709493.
- [54] Dong X, Liao P, Liu X, Yang Z, Wang Y, Zhong W, *et al.* Construction and validation of a reliable disulfidptosis-related lncrnas signature of the subtype, prognostic, and immune landscape in colon cancer. *International Journal of Molecular Sciences*. 2023; 24: 12915.

How to cite this article: Lu Zhang, Yu Li, Jingrui Yang, Xinmiao Xiong, Min Kang, Minmin Yu. Prognostic prediction and immune landscape analysis based on m6A methylation modification and vasculogenic mimicry in cervical cancer. *European Journal of Gynaecological Oncology*. 2025; 46(5): 33-45. doi: 10.22514/ejgo.2025.063.